Measurement 153 (2020) 107398

Contents lists available at ScienceDirect

Measurement

journal homepage: www.elsevier.com/locate/measurement

A first realization of ASTM E3125-17 test procedures for laser scanner performance evaluation

Ling Wang [a,b], Bala Muralikrishnan [b,*], Vincent Lee [b], Prem Rachakonda [b], Daniel Sawyer [b], Joe Gleason [c]

[a] School of Mechanical and Electrical Engineering, China Jiliang University, Hangzhou, Zhejiang Province 310018, People's Republic of China
[b] Dimensional Metrology Group, Sensor Science Division, National Institute of Standards and Technology, Gaithersburg, MD 20899, United States
[c] Bal-tec Inc., Los Angeles, CA 90011, United States

ARTICLE INFO

Article history:
Received 27 August 2019
Received in revised form 25 October 2019
Accepted 13 December 2019
Available online 15 December 2019

Keywords:
ASTM E3125-17 standard
Terrestrial Laser Scanners
Performance evaluation
Two-face tests
Point-to-point tests

ABSTRACT

Spherical coordinate three-dimensional (3D) imaging systems, such as Terrestrial Laser Scanners (TLS), are already used widely in different fields. Their measurement performance evaluation is a topic of active research. In 2017, the first comprehensive documentary standard describing performance evaluation methods and procedures for TLS systems, the ASTM E3125-17, was released. In this paper, we report on the first realization of the test procedures per that standard. We briefly discuss the test procedures and then describe the materials and methods used to realize the tests. We then discuss the test measurands (the quantities of interest in the testing procedure), present the test values (the measured values of the test measurands), and the test value uncertainties (uncertainties in the testing process, which is typically the uncertainty in the reference length). The work described in this paper will serve as a useful reference for understanding and implementing the ASTM E3125-17 standard.

Published by Elsevier Ltd.

1. Introduction

Spherical coordinate three-dimensional (3D) imaging systems play a key role in many fields including historical preservation, archiving, reverse engineering, geographic modeling, dimensional metrology and assembly of large structures in engineering. A Terrestrial Laser Scanner (TLS) is one of the most widely used 3D imaging instruments, collecting point cloud data of surfaces rapidly. Manufacturers may need to evaluate the performance of TLSs so that they can develop specifications for their instruments, while users need to compare different instruments or for testing them in order to ensure that they meet specifications. Additionally, TLS performance will likely deteriorate over time due to instrument drift, vibration, and wear and tear. As a result, performance evaluation is very important for TLS users and manufacturers.

In the literature, there exist a large number of papers on TLS performance evaluation. Hiremagalur et al. [4] proposed a set of vendor-neutral standard test protocols for the performance evaluation of 3D laser scanners, which can be conducted by users in easily accessible facilities. Gumus and Erkaya [3] compared geometric and nominal measurements of 3D models obtained by scanning object surfaces using a TLS Trimble-Mensi GS 100 with the measurements of real reference models. Tsakiri et al. [14] proposed a test procedure that can assess the overall achievable precision for a TLS based on the ISO standard (ISO-17123-(1-8)) for specifications of geodetic instruments. Incekara and Seker [5] analyzed the difference in accuracy of point cloud data obtained via close-range photogrammetry (CRP) and via TLS. Beraldin et al. [2] presented an experimental procedure and results in order to evaluate the measurement uncertainty for medium range (2 m–100 m) laser scanners, using a custom-made reference test object. Li et al. [6] calibrated mounting angle errors of a TLS based on a self-calibration model. Muralikrishnan et al. [7] described a geometric error model for large volume laser scanners in detail, and they also explored the sensitivity of different two-face and volumetric length tests for each term in the model. In order to evaluate the distance measurement performance of laser scanners, Muralikrishnan et al. [8] also compared point-to-point distances obtained by a TLS under tests against those obtained by a reference instrument. Additionally, Muralikrishnan et al. [10,11] designed a new artifact (a plate-sphere target) for the quick and efficient realization of the relative-range error tests.

Based on the previous work and a continuation of the ASTM E57 committee effort, TLS users, TLS manufacturers, and National Metrology Institutes developed the ASTM E3125-17 standard [1,12] for laser scanner performance evaluation in 2017. This standard was developed for spherical coordinate 3D imaging systems. There are two sets of required tests in this standard, two-face tests

* Corresponding author.
E-mail address: bala.muralikrishnan@nist.gov (B. Muralikrishnan).

https://doi.org/10.1016/j.measurement.2019.107398
0263-2241/Published by Elsevier Ltd.

and point-to-point distance tests. The point-to-point distance tests can be further categorized as symmetric tests, asymmetric tests, the inside test, relative-range tests, and user-selected tests. In this paper, we will describe the first realization of these ASTM E3125-17 test procedures for TLS performance evaluation including the materials and methods used, the test measurands (the quantities of interest in the testing procedure), present the test values (the measured values of the test measurands), and the test value uncertainties (uncertainties in the testing process, which is typically the uncertainty in the reference length). We used a laser tracker (LT) as the reference instrument in this paper.

The organization of this paper is as follows: we briefly introduce the required ASTM E3125-17 tests in Section 2 and then describe the materials and methods used in our realization in Section 3. We discuss the test results and the uncertainty budgets in Section 4 and present conclusions in Section 5.

2. ASTM E3125-17 test procedures

The test methods in the ASTM E3125-17 standard are developed for the performance evaluation of laser-based, scanning, time-of-flight, single-detector 3D imaging systems in the medium-range (2 m–150 m). In particular, the requirements and test procedures given in this standard can be used for evaluating the derived-point to derived-point distance measurement performance throughout the work volume of these systems, which are able to rapidly produce a point cloud data of an object of interest. The derived-point is a singular point that is calculated by processing a cloud of points which represents a geometric object (a sphere center). The test methods of the ASTM E3125-17 standard are designed based on the systematic error models described by Muralikrishnan et al. [7] for spherical coordinate 3D imaging systems. This standard should not be applied to non-spherical coordinate 3D imaging systems as the error sources and sensitivity of these error sources may be different for these systems. In the rest of this section, we will give a brief introduction of the test procedures in the ASTM E3125-17 standard.

2.1. Two-face tests

Many TLSs can measure targets in two faces, i.e. front-face and back-face. As shown in Fig. 1(a), a TLS instrument has a laser source, and a spinning prism mirror mounted on a platform that can rotate around the vertical Z axis. The spinning mirror can rotate around the T axis. The front-face of the TLS may be arbitrarily defined based on the zenith angle of the spinning prism mirror that directs the laser beam. For example, if the laser beam emerges when the zenith angle is between 0° and 180°, that face of the instrument may be noted as the front-face. As shown in Fig. 1(a), if it is considered that the target P is measured by front-face when the platform and the mirror are in the position shown in this figure, then the target P is measured by back-face when the platform rotates 180° and the mirror rotates correspondingly around the T axis for pointing the laser beam at the target P again.

In the standard, a two-face test involves measurement of a sphere in the front-face mode followed immediately by a measurement of the same sphere in the back-face mode. The apparent distance between the front-face and back-face coordinates of the best-fit center of the target is the test measurand, i.e., the quantity of interest in the test. As shown in Fig. 1, the two-face test procedure requires scanning three spheres (A, B, and C). Three different spheres may be mounted on a bar (see Fig. 1(b)), or a single sphere may be moved to three different positions. Alternately, one sphere target and two mirrors may be used as shown in Fig. 1(c). In this case, a single sphere is measured directly, as well as through reflections from two mirrors to realize the different elevation angles. The two mirrors should have flatness and optical properties that are compatible with the laser output (wavelength, polarization, frequency, etc.) from the TLS. The errors introduced by the mirrors should be considered in the determination of the uncertainty in the test value.

In the two-face test, the angle ϕ in Fig. 1 should be 45° ± 10°. Two-face tests are required to be performed at two different distances ($d \leq 10$ m and $d \geq 20$ m) and two orientations (θ and $\theta + 90°$), where θ is arbitrarily chosen. Therefore, a total of 3 (spheres) × 2 (distances) × 2 (orientations) = 12 two-face measurements are performed.

The standard requires that TLS settings and operating modes be within the rated conditions and be chosen in order to obtain a minimum of 300 measured points on the sphere target after point selection. The comprehensive description of the point selection can be found in Rachakonda et al. [13].

2.2. Point-to-point distance tests

A point-to-point distance test involves the measurement of the distance between two targets using both the TLS and the LT. The error in the measured distance is the test measurand, i.e., the quantity of interest in the test. In the ASTM E3125-17 standard, the point-to-point distance tests are classified as symmetric, asymmetric, inside, relative-range, and user selected tests. Sphere targets are used for the all point-to-point distance tests except the relative-range tests, which requires the use of plate targets. The standard requires TLS settings and operating modes be within the rated conditions and be chosen in order to obtain a minimum of 300 measured points on the sphere target and 100 points on the plate target after point selection.

2.2.1. Symmetric tests

In the symmetric tests, the point-to point distances between four pairs of sphere targets, A_iB_i (i = 1, 2, 3, and 4) as shown in Fig. 2, are calculated. Each pair of spheres is symmetrically placed with respect to the TLS and is also measured in two orientations of the TLS (the two azimuth angles are θ and $\theta + 90°$ as shown in Fig. 2). Therefore, the symmetric tests involve eight measurements, all in the front-face mode or all in the back-face mode. The standard does not restrict the use of various artifact designs, other than geometric shape, to realize these tests. The lengths between the pairs of sphere targets A_iB_i (i = 1, 2, 3, and 4) may be obtained in different ways including a) four pairs of spheres on four different scale bars, or b) the same pair of spheres on a single scale bar rotated at four different angles, or c) a grid of sphere targets mounted stably on rails or on walls. In order to evaluate the performance within the work volume of the TLS, the symmetric tests require the sweep angles $\angle A_iOB_i$ (i = 1, 2, 3, and 4 for the horizontal, vertical, left diagonal, and right diagonal pairs, respectively, as shown in Fig. 2) be larger than 80°. The line A_1B_1 is horizontal and at the same height as the TLS. The standard allows the user to freely select any combination of distance between targets and distance from the TLS that meets the angular sweep requirements as long as those values are within the rated conditions of the TLS.

2.2.2. Asymmetric tests

In the asymmetric tests, the point-to-point distances between three pairs of sphere targets, A_1C (or A_2C) and B_1C (or B_2C) in Fig. 3(a) and A_1B_1 (or A_1B_2) in Fig. 3(b), are calculated. Each pair of sphere targets are scanned at two orientations of the TLS (the two azimuth angles are θ and $\theta + 90°$ as shown in Fig. 3). As a result, there are a total of six asymmetric point-to-point distance tests. For the horizontal or vertical asymmetric lengths shown in Fig. 3 (a), the angular sweep $\angle A_iOC$ or $\angle B_iOC$ (i = 1, 2) between the two

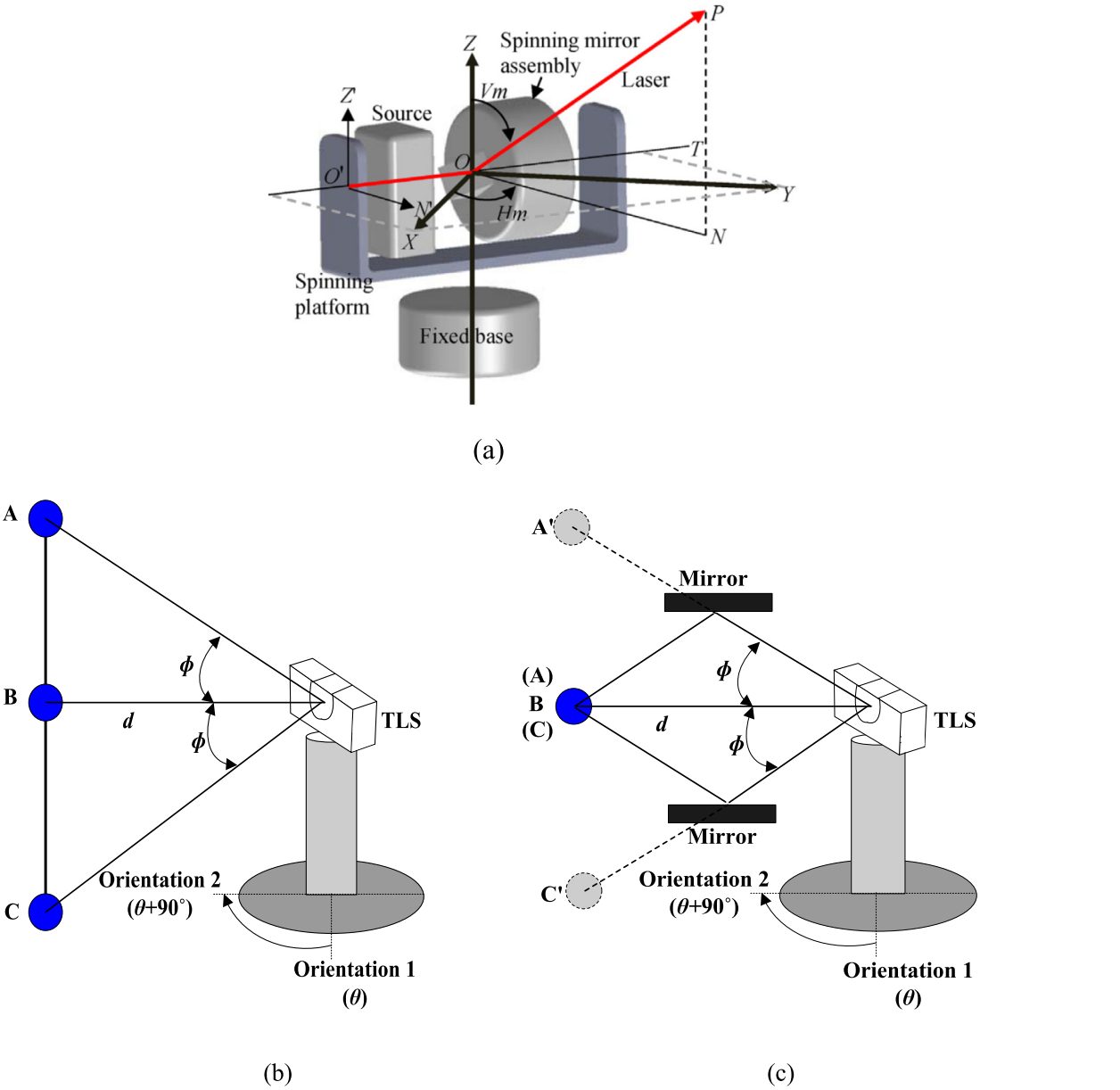

Fig. 1. (a) Two-face measurement of a target (Muralikrishnan et al. [7]), (b) Two-face testing on three targets A, B, and C, (c) Two-face measurements using mirrors and one target.

targets must be at least 40°. Similarly, for the diagonal lengths shown in Fig. 3(b), the angular sweep $\angle A_1OP$ and $\angle B_1OP$ (or $\angle B_2OP$) must be also at least 40°, and the inclination angle $\angle A_1B_1P$ (or $\angle A_1B_2P$) is nominally 45°. The standard allows the user to freely select any combination of distances between targets and distances from the TLS that meets the angular sweep requirements as long as those values are within the rated conditions of the TLS.

2.2.3. Inside test

In the inside test, two sphere targets are placed so that their centers are collinear with the origin of the TLS. They are at the same height as the TLS, on either side of the TLS, and nominally equidistant from the TLS, see Fig. 4. The error in the distance between the spheres is the test measurand. The standard presents collinear quantification requirements: if the azimuth angle of the sphere target A is θ_A, then the azimuth angle of the sphere target B should be within θ_A + 180° ± 10°, and the zenith angles of both sphere targets A and B should be within 90° ± 10°.

Additionally, one of the targets is scanned in the front-face mode while the other target is scanned in the back-face mode, either sequentially or simultaneously. However, if the TLS cannot measure targets in the back-face mode, the standard permits measurements of both targets in the front-face mode.

2.2.4. Relative-range tests

In the relative-range test shown in Fig. 5, a planar target is scanned sequentially at four positions (A, B, C, and D) along a ranging axis direction of the TLS. The position A is considered the reference position, and the positions B, C, and D are the test positions. Three distances, d_{AB}, d_{AC}, and d_{AD}, are calculated as shown in Fig. 5, for the reference and test instruments. The errors in those three distances are the test measurands. It is permitted to use different planar targets at the reference and test positions in this standard.

As shown in Fig. 5, the center of the target at the three test positions (B, C, and D), the reference position (A), and the TLS origin (O)

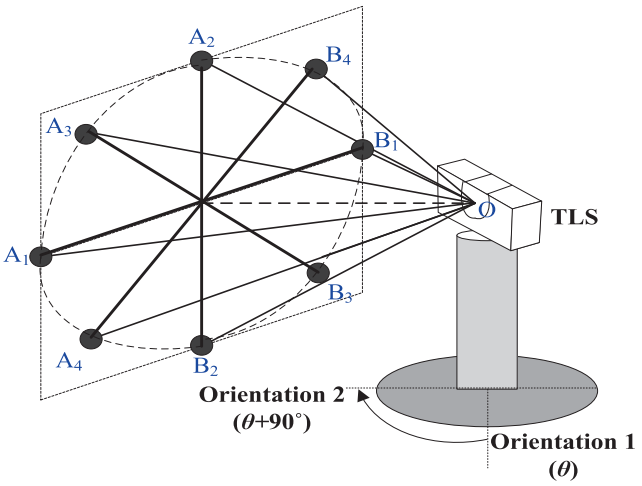

Fig. 2. Layout of symmetric tests of the ASTM E3125-17 standard.

should be nominally collinear. In particular, the standard requires that the target center at the test positions should not be offset by more than 0.2 m from the measurement axis, which is the line joining the TLS origin *O* and the target center at the reference position A. Furthermore, it is also recommended that the point selection region of the planar target should not span more than ±10° along the azimuth or elevation angle directions of the TLS at the positions A, B, C, and D.

2.2.5. User-selected tests

The ASTM E3125-17 standard requires users to perform two additional point-to-point distance tests that are proposed by the TLS user. The users may choose to perform additional repeats of any of the point-to-point distance tests described in the symmetric, asymmetric, inside, and relative-range tests above as the user-selected tests. The users may also choose to perform other point-to-point distance tests anywhere in the measurement volume (including along the ranging direction) if the tests meet the rated operating conditions of the TLS. We do not discuss these tests in this paper as they are specific to each user.

2.2.6. Data processing

The ASTM E3125-17 standard also contains methods to calculate the coordinates of the derived-point for sphere and plate targets. Comprehensive description and MATLAB/Python code for the center coordinate calculation for sphere targets can be found in Rachakonda et al. [13].

3. Materials and methods

3.1. Mirror frame and scanning sphere for two-face tests

The two-face tests are realized using an aluminum sphere target of nominal diameter 200 mm, with a dull gray matte finish. A special apparatus with two high quality plane mirrors mounted on a frame as shown in Fig. 6 was used to measure this sphere. The frame-mirror setup allows the TLS to scan the sphere target directly and also through the reflections from the two mirrors simultaneously as shown in Fig. 1(c)

TLS settings and operating modes within rated conditions are chosen in order to obtain a minimum of 300 measured points on the sphere target after point selection. During the tests, we changed the TLS orientation and the sphere distance, and scanned the sphere and its reflections in the two mirrors based on the requirements given in Section 2.1 of ASTM E3125-17.

3.2. Three-sphere scale bar for symmetric and asymmetric length tests

We use a scale bar with three spheres for realizing the symmetric and asymmetric length tests in ASTM E3125-17. As shown in Fig. 7(a) and (b), the scale bar can be rotated when mounted on a stand. The length of the scale bar is about 2.3 m, and it is made of carbon fiber tube with a rectangular cross section. At each end and at the middle of the scale bar, specialized aluminum spheres of nominal diameter 100 mm are mounted. The surface of the spheres has a dull gray matte finish. In order to reduce the effect of the bar on the sphere measurements during scanning, the scale bar is covered with a layer of black, laser absorbing fabric over its entire surface except the region containing the three spheres. Each sphere is hollow as shown in Fig. 7(c), with a kinematic nest located inside that allows a 38.1 mm (1.5 in) spherically mounted retro-reflector (SMR) to be centrally placed. By design, the sphere center is coincident with the center of the inner SMR. Therefore, we can use an LT for calibrating the distances between the centers of the three spheres, see Wang et al. [15]. In the measurements we performed, the scale bar was positioned and oriented so as to meet the requirements of the symmetric and asymmetric length tests in ASTM E3125-17.

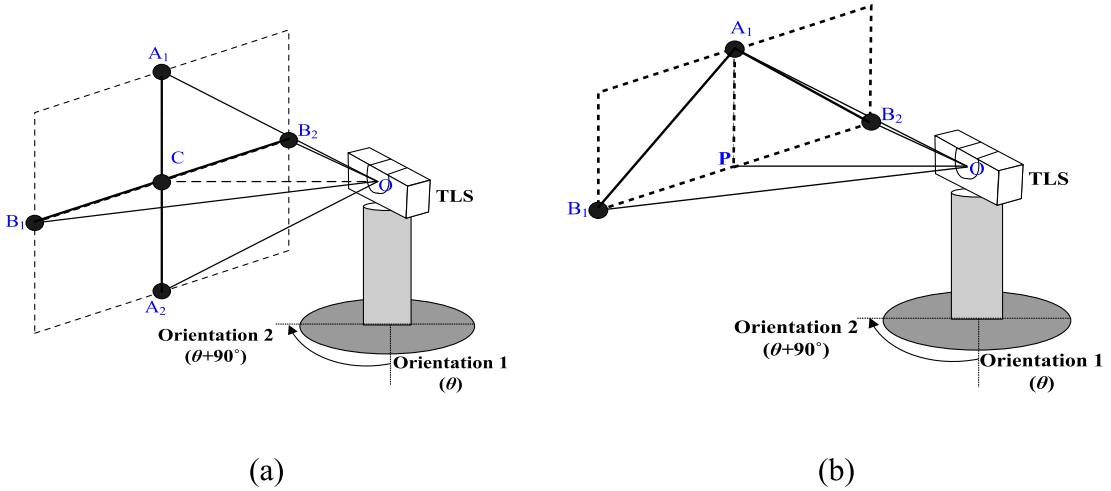

Fig. 3. Layout of asymmetric tests of the ASTM E3125-17 standard.

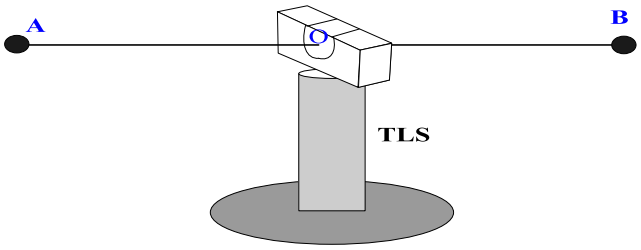

Fig. 4. Layout of the inside test of the ASTM E3125-17 standard [1]

3.3. Stands and scanning spheres for inside test

To realize the inside test, two scanning spheres (S1 and S2) are placed 6 m apart from each other, collinear with and on either side of the TLS, equidistant from and at the same height as the TLS. Because the spheres are both facing the TLS as shown in Fig. 8, the kinematic nests on the back-side of the spheres point in opposite directions and are not in line-of-sight (LOS) from a single LT position. We therefore calibrate the sphere center-to-center distance from two positions of the LT as described below:

(1) We place three registration nests R1, R2, and R3, as shown in Fig. 8. The nests R1 and R2 are located near S1 and S2, respectively.
(2) With the LT at position 1, we measure the coordinates of R1, R2, R3, and S1.
(3) We move the LT to position 2 and measure the coordinates of R1, R2, R3, and S2.
(4) We then establish the locations of S1 and S2 in a common coordinate system determined from the measurements of nests R1, R2, and R3 from the two LT positions.
(5) We then calculate the distance between S1 and S2 in the previously established coordinate system. This is the reference value for the distance between the sphere targets.
(6) We then scan the two spheres using the TLS and determine the distance between the centers of the sphere targets.
(7) We finally calculate the difference between the distances determined by the TLS and the LT as the test value.

There are several details to note with regard to the steps outlined above. In order to reduce the effect of error sources associated with the LT, the measurements in steps 2 and 3 are performed from four azimuth orientations of the LT, i.e., the LT is rotated by 90° between each set of measurements. There are many ways to determine the common coordinate system using the measured registration points. We calculate the average distance between any pair of registration points from the measurements made from the four azimuth LT orientations and the two LT positions. We then assume that the nest R1 is the origin, R2 is located on the *X* axis, and R3 is located on the *XY* plane. As a result, we can determine the remaining unknown coordinates of R2 (the *X* coordinate) and R3 (the *X* and *Y* coordinates) based on the previously determined distances between R1-R2, R1-R3, and R2-R3. We refer to this as the registration-based method for distance calibration.

In order to validate this method, we replace the spheres S1 and S2 with 38.1 mm (1.5 in) SMR validation nests T1 and T2. We follow the procedure outlined above to determine the distance between the validation nests T1 and T2, i.e. the distance between T1 and T2 could be determined by the registration-based method above (represented as $L_{T1T2,reg}$). On the other hand, we then perform a LOS measurement of the validation nests T1 and T2 by aligning the LT to be collinear with T1 and T2, and the result is represented as $L_{T1T2,LOS}$. This LOS measured result $L_{T1T2,LOS}$ is considered to represent the true value of the distance between nests T1 and T2. We then establish that the registration-based measurement result $L_{T1T2,reg}$ is within a few micrometers of the LOS measurement result $L_{T1T2,LOS}$. Therefore, we can consider this a valid method for the calibration of the distance between S1 and S2 based on the registration-based method above.

3.4. Plate-sphere artifact for relative-range tests

We use a plate-sphere artifact for performing the relative-range tests described in the ASTM E3125-17 standard. The 304.8 mm × 304.8 mm × 25.4 mm (12 in × 12 in × 1 in) plate is made of aluminum and is shown in Fig. 9(b). Additionally, two spheres of diameter 100 mm are mounted on the sides of the plate. The spheres are hollow with a nest located inside that allows a 38.1 mm (1.5 in) spherically mounted SMR to be centrally placed, as shown in Fig. 9(c). By design, the center of the two spheres are on the plane defined by the front surface of the plate. In the tests, the TLS is located on the front side of the plate-sphere target and

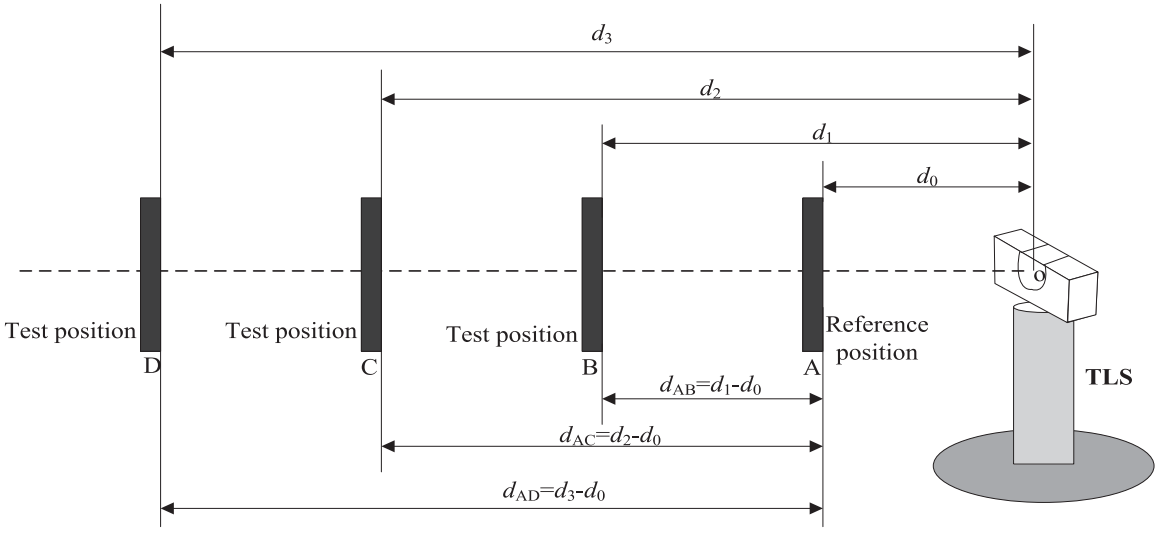

Fig. 5. Layout of relative-range test of the ASTM E3125-17 standard.

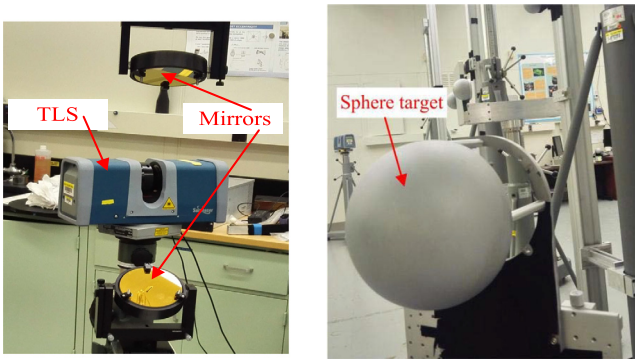

Fig. 6. Sphere target, mirrors and TLS for two-face tests.

the LT is located at the back side of the target. The target, the TLS, and the LT are nominally collinear.

In order to find a common point on the plane that is measured by both the TLS and the LT, the two spheres are used as fiducials. Thus, careful alignment of the plate is no longer necessary for ensuring that both the TLS and the LT measure the same point in space. For the detailed description of this artifact, see Muralikrishnan et al. [10].

At each position of the plate target (the positions A, B, C, and D, shown in Fig. 5), we use the LT to measure the centers of the two spheres, then average the two measured coordinates as the reference point for the center of the plate. Then, the distances between the reference and test points ($d_{\mathrm{Ai,ref}}$, i = B, C, and D) can be calculated.

At each position of the plate target, we scan both the plate and the two spheres using the TLS. Then the average of the two sphere center coordinates is determined and projected onto the plane that is defined by the point cloud data of the plate. As a result, the distances between the projected points ($d_{\mathrm{Ai,proj}}$, i = B, C, and D) is derived. Finally, we can evaluate the TLS performance by comparing the TLS distances $d_{\mathrm{Ai,proj}}$ with the LT distances $d_{\mathrm{Ai,ref}}$ (i = B, C, and D).

4. Results and discussions

Based on the requirements in the ASTM E3125-17 standard and the materials and methods described earlier, we report the results from the first realization of the ASTM E3125-17 test procedures in this section. We also present a discussion of the uncertainties in the test values.

4.1. Two-face tests

4.1.1. Results

In the two-face tests, let the derived coordinate of the sphere center measured by the TLS front-face be (r_1, θ_1, ϕ_1) and the derived coordinate of the same sphere center by the TLS back-face be (r_2, θ_2, ϕ_2), where r_1 and r_2 are the range values, θ_1 and θ_2 are the azimuth angles in radians, and ϕ_1 and ϕ_2 are the elevation angles in radians. Then, based on the standard, the test measurand is the two-face error for each sphere center, $E_{two\text{-}face}$, and is calculated as follows:

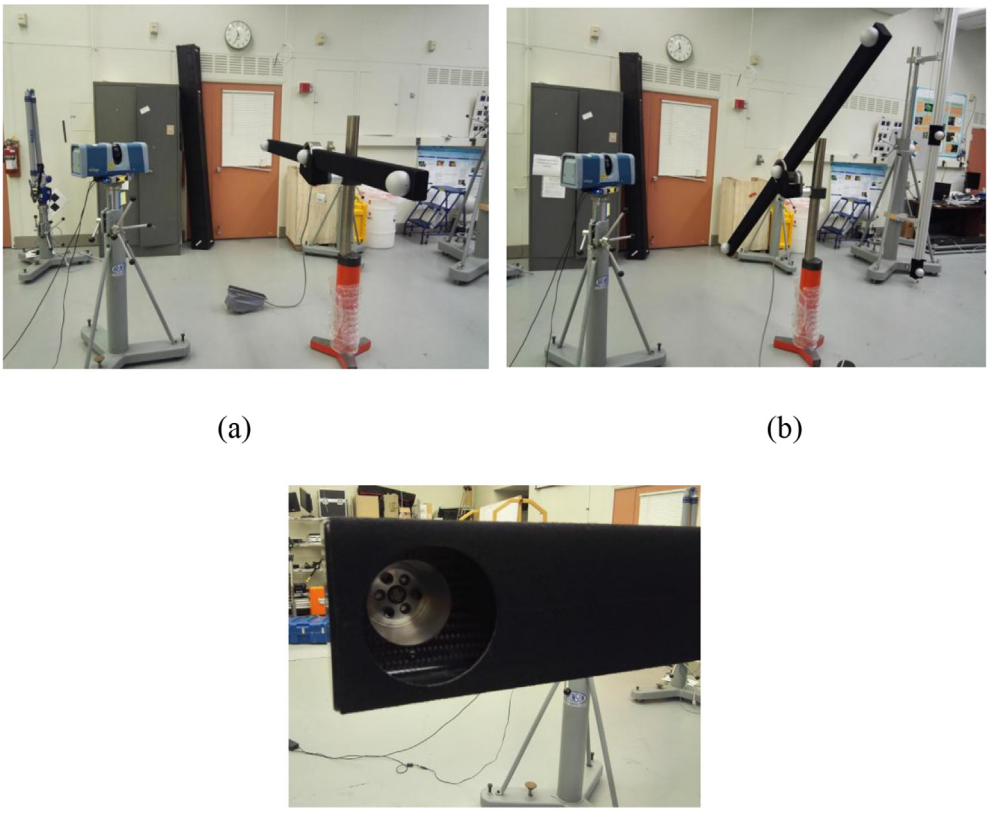

Fig. 7. Different views of the three-sphere scale bar for symmetric and asymmetric tests.

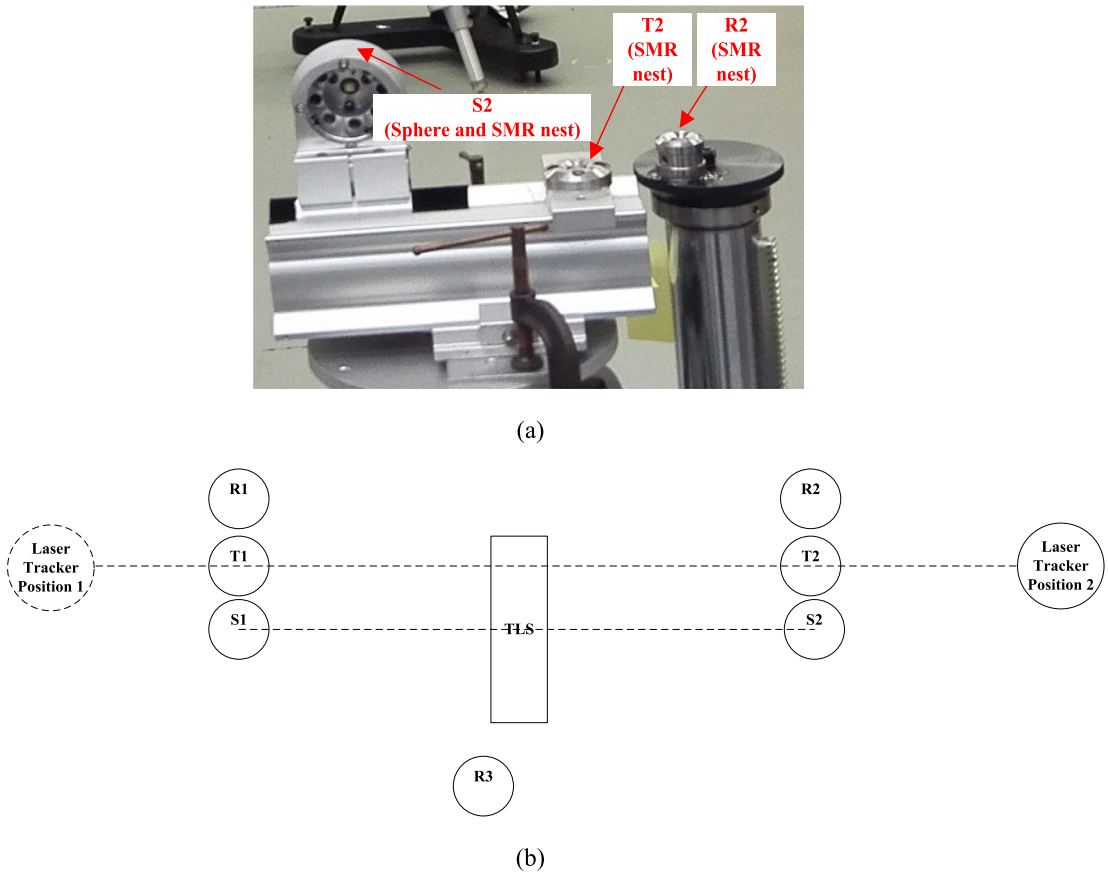

Fig. 8. Stands and scanning spheres for the inside test: (a) spheres and nests used in the test (b) layout of the artifacts and instrument.

$$E_{two-face} = r_1 \times \sqrt{(\phi_1 - \phi_2)^2 + ((\theta_1 - \theta_2) \times \cos(\phi_1))^2} \quad (1)$$

The test values, i.e., the two-face test results, for the TLS under study are given in Table 1. Most of the errors are less than 0.6 mm. The two-face error is generally larger when the sphere target is farther away from the scanner. The two largest errors recorded are 0.890 mm and 1.151 mm when the sphere target is about 20 m from the TLS and at elevation angle of approximately −45°. TLS systems have several geometric and optical misalignment sources that result in errors in the measured point coordinates (Muralikrishnan et al. [7]. There are 10 different model parameters that contribute to errors in the measured vertical angle, five of which are sensitive to two-face testing. Linear combinations of these parameters can produce different sets of two-face errors; it is possible that one such combination produced the observed set of two-face errors. A complete analysis of the model parameters and their relationship to the observed errors is beyond the scope of this work The number of measured points on the sphere targets after point selection are more than 2800 and 1100 when the distances between the three spheres and the TLS are about 8 m and 20 m, respectively, thus satisfying the minimum point requirement of 300.

4.1.2. Uncertainty

If there are any perturbations to the target position between the front-face and back-face measurements, that will contribute to an uncertainty to the test value. Because the front-face and back-face measurements occur within a few minutes of each other, it is reasonable to assume that the uncertainty is negligible for the errors of two-face test values shown in Table 1.

4.2. Symmetric and asymmetric tests

4.2.1. Results

In the symmetric length tests, the three-sphere scale bar is scanned by the TLS, based on the requirements given in Section 2.2. The test values, i.e., the length errors, are shown in Table 2. In the tests, we ensured that the sweep angles $\angle A_i OB_i$ (i = 1, 2, 3, and 4) shown in Fig. 2 were close to 90°. The calibration of the scale bar length is discussed in Wang et al. [15]. Table 2 shows that the maximum length error is −0.443 mm among the eight symmetric tests for the 2.3 m long scale bar. As discussed in the Section 4.1.1, our objective is only to describe materials and methods to perform the ASTM E3125-17 tests. We have not attempted to fit the observed errors to a TLS error model to explain the cause.

We used the same three-sphere scale bar for realizing the asymmetric length tests as well. The sphere in the middle of the scale bar and one of the two end spheres were used for the asymmetric horizontal and vertical length tests, and the two end spheres were used for the asymmetric diagonal test. Table 3 shows the maximum error in the asymmetric length tests, which was about −0.226 mm when the scale bar is oriented in the asymmetrical vertical position.

As shown in Tables 2 and 3, the errors in the symmetric length tests are larger than that in the asymmetric length tests. The symmetrical length tests are sensitive to certain error sources such as a laser beam that is offset from ideal position whereas symmetric length tests capture other error sources such as out-of-squareness between axes, encoder errors, etc. The fact that the asymmetric length tests produced smaller errors than symmetric tests indicate that encoder errors are perhaps more dominant in our TLS.

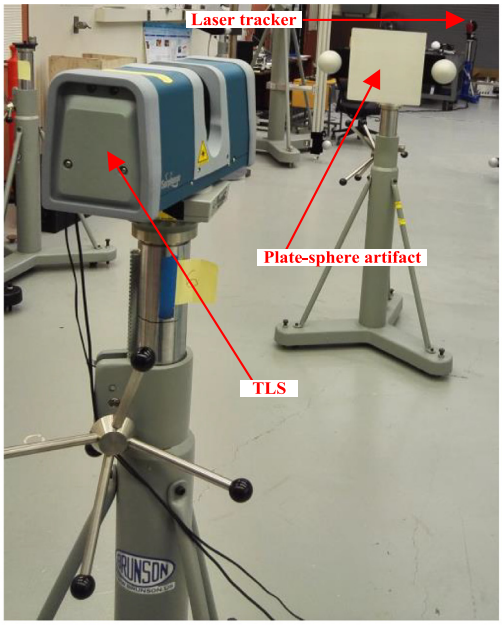

(a)

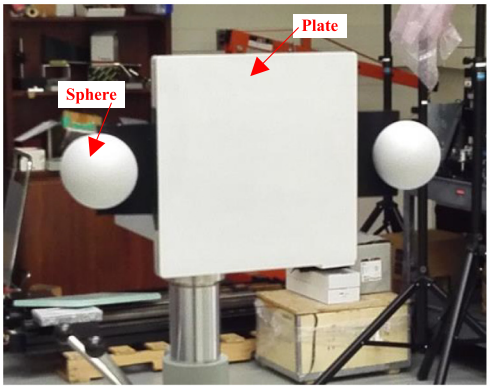

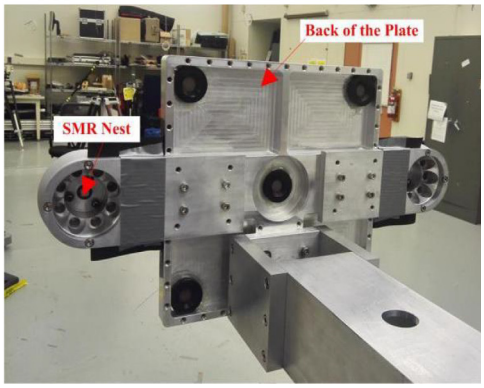

(b) (c)

Fig. 9. Plate-sphere for relative-range tests (a) Layout of the tests (b) Front view (c) Back view.

Table 1
Result of two-face tests.

Distances of sphere target from TLS (m)	TLS Orientation (°)	Test values, i.e., errors of two-face tests for each sphere $E_{two\text{-}face}$ (mm)		
		Sphere A	Sphere B	Sphere C
8	0	0.276	0.235	0.492
8	90	0.369	0.292	0.428
20	0	0.594	0.375	1.151
20	90	0.480	0.288	0.890

Note: The test values corresponding to spheres A and C are obtained through reflections from the mirrors, see Fig. 1(c).

4.2.2. Uncertainty

We calibrated the three-sphere scale bar length by the LOS method using the LT. In the LOS method, the laser beam of the laser tracker is aligned along the line joining the targets directly or through a mirror. Thus, the distances among these targets (two or more) that are nominally collinear with the laser tracker could be measured. In this study, the difference in azimuth and elevation angles of the targets are typically smaller than 0.05°. For the detailed description of the LOS method, refer Wang et al., [15]. The uncertainty budget of the calibrated bar length by the LOS method is detailed as follows:

Table 2
Result of symmetric tests.

Scale bar orientation from Fig. 2	TLS orientation (°)	Scale bar length measured by TLS (mm)	Calibrated scale bar length (mm)	Length errors (mm)
Symmetric horizontal A_1B_1	0	2299.182	2299.625	−0.443
Symmetric horizontal A_1B_1	90	2299.271		−0.354
Symmetric vertical A_2B_2	0	2299.249		−0.376
Symmetric vertical A_2B_2	90	2299.264		−0.361
Symmetric left diagonal A_3B_3	0	2299.462		−0.163
Symmetric left diagonal A_3B_3	90	2299.531		−0.094
Symmetric right diagonal A_4B_4	0	2299.209		−0.416
Symmetric right diagonal A_4B_4	90	2299.230		−0.395

Table 3
Result of asymmetric tests.

Scale bar orientation from Fig. 3	TLS Orientation (°)	Scale bar length measured by TLS (mm)	Calibrated scale bar length (mm)	Length errors (mm)
Asymmetric horizontal B_1C in Fig. 3(a)	0	1149.612	1149.750	−0.138
Asymmetric horizontal B_1C in Fig. 3(a)	90	1149.632	1149.750	−0.118
Asymmetric vertical A_1C in Fig. 3(a)	0	1149.534	1149.750	−0.216
Asymmetric vertical A_1C in Fig. 3(a)	90	1149.524	1149.750	−0.226
Asymmetric diagonal A_1B_1 in Fig. 3(b)	0	2299.616	2299.625	−0.134
Asymmetric diagonal A_1B_1 in Fig. 3(b)	90	2299.644	2299.625	0.106

(1) LT contribution: The ADM mode of the LT has a specification of 10 μm accuracy over the measurement range. It is assumed that any value within this specification is equally probable, and the uncertainty in the measurement of any target is 10 μm/$\sqrt{3}$ ≈ 6 μm along the ranging direction. Moreover, the temperature change in our lab is kept within a range of ±0.5 °C, which is within the rated operating conditions provided by the LT manufacturer. Therefore, we do not consider the effect of temperature on the refractive index of air separately.
(2) Concentricity between the SMR mechanical center and the outer surface of the scanning sphere target: This concentricity value was obtained from measurements on a CMM. The standard uncertainty due to this term is 5 μm.
(3) Concentricity between the SMR mechanical and optical centers: based on the data given by the SMR manufacturer, the concentricity of the maximum distance between mechanical and optical centers of the SMR used in the study is 2.5 μm. It is assumed that any value within this bound is equally probable. Then the standard uncertainty in the measured coordinate is 2.5 μm/$\sqrt{3}$ ≈ 1.4 μm.
(4) Thermal effect: in the tests, it is assumed there exists ±0.5 °C fluctuation of the temperature in the lab, and any value within the bound is equally probable. The thermal expansion coefficient of carbon fiber is 2×10^{-6}/°C. As a result, the standard uncertainty of thermal effects for the 2.3 m length is 1 μm.
(5) Scale bar orientation: Because the length of the scale bar changes from the horizontal to the vertical orientation and the LOS calibration was only performed in the horizontal orientation, we account for this term through an experimentally determined standard uncertainty of 10 μm.

Because two sphere centers are involved, the standard uncertainties of the first three items above for the coordinate of single sphere center are multiplied by the factor $\sqrt{2}$ when calculating the scale bar length uncertainty. Table 4 shows the uncertainty budget for the calibrated scale bar length. The k = 2 expanded uncertainty in the length of the scale bar is 32 μm.

4.3. Inside test

4.3.1. Results

The inside test is described in Section 2.3. As shown in Table 5, the test value, i.e., the error of the inside test, is −0.147 mm. This is a constant ranging error in the instrument and will affect all range measurements.

4.3.2. Uncertainty

The uncertainty budget for the inside test is described here.

(1) LT contribution: based on our experimental measurements, one standard deviation repeatability of the angular axis of the LT is about 0.0001°. When the nominal distance between the LT at position 1 and the target R2 in Fig. 8(b) is about 7 m, the standard uncertainty is about 12 μm. When the nominal distance between the LT at position 1 and the target R1 in Fig. 8(c) is about 1 m, the standard uncertainty is about 2 μm. These parameters are similar with those described in Muralikrishnan et al. [9]. We therefore use their uncertainty result of 11 μm for the LT contribution in the inside test based on a Monte Carlo Simulation they have performed.
(2) Concentricity between the SMR mechanical center and the outer surface of the scanning sphere target: The concentricity of the scanning spheres is measured by a CMM. The standard uncertainty due to this term is 5 μm.

Table 4
Uncertainty budget for the scale bar length by the LOS method.

Uncertainty Sources	Standard uncertainty (μm)
Standard uncertainty in the length due to LT errors	$6\sqrt{2}$
Concentricity between the SMR mechanical center and the outer surface of the scanning sphere target	$5\sqrt{2}$
Concentricity between the SMR mechanical and optical centers	$1.4\sqrt{2}$
Thermal effects	1
Scale bar orientation	10
Combined standard uncertainty	**16**
Expanded uncertainty (k = 2)	**32**

Table 5
Distance result of S1-S2 in inside test (mm).

Reference distance by LT using the registration-based method (Fig. 8)	Measured distance by TLS	Distance error
4621.138	4620.991	−0.147

(3) Concentricity between the SMR mechanical and optical centers: based on the data given by the SMR manufacturer, the concentricity of the maximum distance between physical and optical centers of the SMR used in the study is 2.5 μm. It is assumed that any value within this bound is equally probable. Then the standard uncertainty in the measured coordinate is 2.5 μm/$\sqrt{3}$ ≈ 1.4 μm.
(4) Besides the three error sources given above, there is still the thermal effects of the concrete ground in the lab. It is assumed there exists ±0.5 °C fluctuation of the temperature in the lab, and the thermal expansion coefficient of the concrete is 12 × 10^{-6}/°C. Therefore, the standard uncertainty is calculated to be 0.5 × 12 × 4.62/$\sqrt{3}$ = 16 μm for a 4.62 m length on the ground.

Because two sphere centers are involved when calculating the scale bar length, the standard uncertainties of some items above for the coordinate of single sphere center are multiplied by the factor$\sqrt{2}$ as shown in Table 6. The combined standard uncertainty is 20 μm, and the expanded uncertainty (k = 2) is 40 μm.

As described in Section 3.3 we perform a validation experiment by establishing the nests T1 and T2 near the spheres S1 and S2. The registration-based length determined by the LT between the nests T1 and T2 are then compared to the LOS method of the LT. Table 7 shows the results of this experiment. The two methods agree to within 5 μm, which is well under the claimed uncertainty in Table 6.

4.4. Relative-range tests

4.4.1. Results

The relative range tests are discussed in Section 2.4. The test values, i.e., errors in the relative range tests, are presented in Table 8. The three relative-ranges considered in this testing are approximately 2.5 m, 5 m, and 7.5 m. Specifically, the TLS and the LT are separated by a distance of about 14 m. The reference position is located 2 m from the TLS (12 m from the LT), and the three test positions are located at about 4.5 m, 7 m, and 9.5 m from the TLS (9.5 m, 7 m, and 4.5 m from the LT). The errors of the TLS measurements increase with increasing relative-range, and the maximum error of the TLS measurements is 0.131 mm. As required in the standard, we also calculate the RMS index for reporting the dispersion of the measured plate points:

Table 6
Uncertainty budget for the distance between the two scanning spheres in the inside test.

Uncertainty Sources	Standard uncertainty (μm)
Standard uncertainty in the length due to LT errors	11
Concentricity between the SMR mechanical center and the outer surface of the scanning sphere target	$5\sqrt{2}$
Concentricity between the SMR mechanical and optical centers	$1.4\sqrt{2}$
Thermal effects	16
Combined standard uncertainty	**20**
Expanded uncertainty (k = 2)	**40**

Table 7
Validation of the registration-based method (mm).

LOS method	Registration-based method	Difference
4789.065	4789.061	0.004

$$RMS = \sqrt{\frac{\Sigma_{i=1}^{N} q_i^2}{N}} \quad (2)$$

In Eq. (2), q_i is the residual distance of the measured point i to the least-squares best-fit plane based on the plate point cloud, and N is the total number of the measured points of the plate being used for the least-squares fitting. As shown in Table 8, the relative distance errors and the *RMS* results are on the same order of magnitude in the relative-range tests. There were more than 7000 points on the plate at each position after point selection, thus satisfying the requirements in the standard for a minimum of 100 points.

4.4.2. Uncertainty

In our realization of the relative-range tests, the uncertainty budget is given as follows:

- LT contribution: the LT has a specification of 10 μm accuracy over the measurement range. It is also assumed that any value within this specification is equally probable, and the uncertainty in the measurement of the reference position and each test position is 10/$\sqrt{3}$ = 6 μm along the ranging direction.
- Thermal effect: The temperature sensor of the LT only monitors the temperature at one point along the laser path. Because long lengths are measured, the tracker is unable to adequately compensate for the changing thermal environment. Therefore, the uncertainty in range measurements due to temperature fluctuations along the laser path is considered. Assuming ± 1 °C fluctuation in temperature along the laser path with any value inside that bound as equally probable, and with the temperature influence of 1 × 10^{-6}/°C (this is due to the change in refractive index based on Edlén's equation), the standard uncertainty in range measurement at a distance of r meters is $r/\sqrt{3}$ in units of micrometers. The uncertainty in determining the range to the target is the root sum square of the two terms. Thus, it is $\sqrt{\left(r/\sqrt{3}\right)^2 + 6^2}$ in units of micrometers. The uncertainty in the displacement is the root sum square of the uncertainty in the range at two ends of the length.

The uncertainty budgets of the relative-range tests are summarized in Table 9. The standard and expanded uncertainties for the distances AC and AD are smaller than that for AB.

4.5. Conformance decisions

In order to determine whether the TLS conforms with manufacturer specifications when evaluated using the ASTM E3125-17 test procedures, each of the test values in Sections 4.1-4.4 must be less than the manufacturer provided maximum permissible error (MPE) specification. Further, the test value uncertainties also must be smaller than the corresponding MPEs by at least a factor of four. Because this is the first realization of the ASTM E3125-17 test procedures and MPE specifications are not yet available for the TLS evaluated, we cannot determine whether it is within specifications. Our objective in this paper is to show how a manufacturer may realize the ASTM E3125-17 test procedures and potentially determine the MPE specification or how a user may determine if the instrument is in conformance or not.

Table 8
Result of relative-range tests (mm).

Positions j	Distance between positions A and j of the plate measured by TLS, $d_{Ai,proj}$	Distance between positions A and j of the plate measured by LT, $d_{Ai,ref}$	Distance error	*RMS*
j = A	/	/	/	0.092
j = B	2467.533	2467.542	−0.009	0.088
j = C	4998.940	4998.830	0.110	0.115
j = D	7516.878	7516.747	0.131	0.147

Table 9
Uncertainty budgets of the relative-range tests.

Uncertainty Sources	Standard uncertainty for the distance AB (μm)
LT ranging errors at the reference position A	6
LT ranging errors at the test position B	6
Thermal effects at the reference position A	7
Thermal effects at the test position B	5
Combined standard uncertainty	12
Expanded uncertainty (k = 2)	24

5. Conclusions

In this paper, we described the first realization of the ASTM E3125-17 standard for the performance evaluation of a TLS. We provided a brief introduction to the required tests in the standard, the materials and the methods used to realize the tests, the measurands, and the test values. Furthermore, the detailed uncertainty budgets are developed and presented for the test values. These uncertainties, referred to as test value uncertainties, are critically important for assessing the conformance of the test results. The artifacts shown in this paper are choices we made based on the materials available to us; other artifacts to realize the test procedures that meet the specifications in the standard are also acceptable. The main conclusions in this study are as follows: for the TLS in this study, we have the following results: the two-face errors are between 0.2 mm and 1.2 mm, and the uncertainty in those errors may be considered to be negligible; the evaluated errors in the scale bar length tests are less than 0.5 mm, and their expanded uncertainties (k = 2) are 32 μm; the measurement error of the TLS for the inside test is less than 0.15 mm, and its expanded uncertainty is 40 μm; the errors in the relative-range tests are smaller than 0.15 mm, and their expanded uncertainties are 24 μm.

The proposed test methods in the ASTM E3125-17 standard are comprehensive and error-source-oriented. We have provided a set of procedures for users who are interested in performing the tests described in the ASTM E3125-17 standard for evaluating the performance of their TLS system. Wider adoption of this standard will enable more uniform specifications among the various instruments and easier comparison between the various instruments.

Acknowledgements

The authors are grateful to Dr. Meghan Shilling and Ms. Geraldine S. Cheok for carefully reviewing this paper. The author Ling Wang would like to thank the support from the Public Welfare Technology Application Research Project of Zhejiang Province Science and Technology Department (LGG18F030010) and the State Scholarship Fund of China Scholarship Council (No. 201808330612).

Disclaimer

Commercial equipment, materials and software may be identified to adequately specify certain procedures. In no case does such identification imply recommendation or endorsement by the National Institute of Standards and Technology, nor does it imply that the materials, equipment or software identified are necessarily the best available for the purpose.

References

[1] ASTM International, 2017. ASTM E3125-17 Standard Test Method for Evaluating the Point-to-Point Distance Measurement Performance of Spherical Coordinate 3D Imaging Systems in the Medium Range. West Conshohocken, PA; ASTM International, 2017, doi: 10.1520/E3125-17.
[2] J.-A. Beraldin, L. Cournoyer, M. Picard, F. Blais, Proposed procedure for a distance protocol in support of ASTM-E57 standards activities on 3D imaging, Proc. SPIE 7239, Three-Dimensional Imaging, Metrology, 72390S (2009), https://doi.org/10.1117/12.814926.
[3] K. Gumus, H. Erkaya, Analyzing the geometric accuracy of simple shaped reference object models created by terrestrial laser scanners, Int. J. Phys. Sci. 6 (28) (2011) 6529–6536.
[4] J. Hiremagalur, K.S. Yen, T.A. Lasky, B. Ravani, 2009, Testing and Performance Evaluation of Fixed Terrestrial 3D Laser Scanning Systems for Highway Applications. Proceeding of TRB 2009 Annual Meeting, 1-19.
[5] A.H. Incekara, D.Z. Seker, Comparative analyses of the point cloud produced by using close-range photogrammetry and terrestrial laser scanning for rock surface, J. Indian Soc. Remote Sens. 46 (8) (2018) 1243–1253.
[6] X. Li, Y. Li, X. Xie, L. Xu, Terrestrial laser scanner autonomous self-calibration with no prior knowledge of point-clouds, IEEE Sens. J. 18 (22) (2018) 9277–9285.
[7] B. Muralikrishnan, M. Ferrucci, D. Sawyer, et al., Volumetric performance evaluation of a laser scanner based on geometric error model, Precis. Eng. 40 (2015) 139–150.
[8] B. Muralikrishnan, M. Shilling, P. Rachakonda, et al., Toward the development of a documentary standard for derived-point to derived-point distance performance evaluation of spherical coordinate 3D imaging systems, J. Manufact. Syst. 37 (2) (2015) 550–557.
[9] B. Muralikrishnan, P. Rachakonda, M. Shilling, V. Lee, C. Blackburn, D. Sawyer, G. Cheok, L. Cournoyer, Report on the May 2016 ASTM E57.02 instrument runoff at NIST, Part 2 – NIST realization of test procedures and uncertainties in the reference lengths, NISTIR 8153, 2016.
[10] B. Muralikrishnan, P. Rachakonda, V. Lee, M. Shilling, D. Sawyer, G. Cheok, L. Cournoyer, Relative-range error evaluation of terrestrial laser scanners using a plate, a sphere, and a novel dual-sphere-plate target, Measur. Sci. Technol. 111 (2017) 60–68.
[11] B. Muralikrishnan, P. Rachakonda, V. Lee, M. Shilling, D. Sawyer, G. Cheok, L. Cournoyer, J. Gleason, Concept to commercialization of an artifact for evaluating three-dimensional imaging systems per ASTM E3125–17, J. Res. Natl. Instit. Stand. Technol. 123 (2018) 1–7.
[12] P. Rachakonda, B. Muralikrishnan, D.S. Sawyer, Roles and responsibilities of NIST in the development of documentary standards, In: Proceedings of the CMSC, July 23–27, 2018, Reno, NV, USA, 37:1–11.
[13] P. Rachakonda, B. Muralikrishnan, L. Cournoyer, S. Daniel, Software to determine sphere center from terrestrial laser scanner data per ASTM standard E3125-17, J. Res. Natl. Instit. Stand. Technol. 123 (2018), Article No. 123006.
[14] M. Tsakiri, V. Pagounis, O. Arabatzi, Evaluation of a pulsed terrestrial laser scanner based on ISO standards, Surf. Topograp. Metrol. Propert. 3 (2015) 1–10.
[15] L. Wang, B. Muralikrishnan, V. Lee, P. Rachakonda, D. Sawyer, J. Gleason, Methods to calibrate a three-sphere scale bar for laser scanner performance evaluation per the ASTM E3125–17, Measurement, in press.